



**HAL**  
open science

# Optimal Regularization for MR Diffusion Signal Reconstruction

Emmanuel Caruyer, Rachid Deriche

► **To cite this version:**

Emmanuel Caruyer, Rachid Deriche. Optimal Regularization for MR Diffusion Signal Reconstruction. ISBI - 9th IEEE International Symposium on Biomedical Imaging, May 2012, Barcelona, Spain. hal-00660635

**HAL Id: hal-00660635**

**<https://inria.hal.science/hal-00660635>**

Submitted on 17 Jan 2012

**HAL** is a multi-disciplinary open access archive for the deposit and dissemination of scientific research documents, whether they are published or not. The documents may come from teaching and research institutions in France or abroad, or from public or private research centers.

L'archive ouverte pluridisciplinaire **HAL**, est destinée au dépôt et à la diffusion de documents scientifiques de niveau recherche, publiés ou non, émanant des établissements d'enseignement et de recherche français ou étrangers, des laboratoires publics ou privés.

# OPTIMAL REGULARIZATION FOR MR DIFFUSION SIGNAL RECONSTRUCTION

*Emmanuel Caruyer, Rachid Deriche*

Athena Project-Team, Inria Sophia-Antipolis – Méditerranée, France.

## ABSTRACT

In this paper we address two problems related to the parametric reconstruction of the diffusion signal in the complete 3D Q-space. We propose a modified Spherical Polar Fourier (mSPF) basis to naturally impose the continuity of the diffusion signal on the whole space. This mathematical constraint results in a dimension reduction with respect to the original SPF basis. In addition, we derive the expression of a Laplace regularization operator in this basis, and compute optimal regularization weight using generalized cross validation (GCV). Experiments on synthetic and real data show that this regularization leads to a more accurate reconstruction than the commonly used low-pass filters.

**Index Terms**— diffusion MRI, optimal regularization, continuous signal reconstruction, spherical polar Fourier basis.

## 1. INTRODUCTION

In diffusion MRI, the reconstruction of the signal attenuation  $E$  and of the probability of water molecules displacement, known as the ensemble average propagator (EAP), open the way to a better characterization of tissue micro-structure. It is still an extremely challenging task however, due to the large acquisition time demand, and the severe SNR loss at high  $b$  values. The Spherical Polar Fourier (SPF) expansion was recently proposed [1] for the reconstruction of  $E$  from discrete measurements in the Q-space. The elements of this basis have a Gaussian-like radial decay, which enables a good extrapolation outside the sampling domain. However, the basis functions show undesirable oscillations and a discontinuity about the origin. In this work, we propose a method to reconstruct the signal in the complete Q-space, with a special focus on continuity and regularization. We derive a modified SPF basis (mSPF) to reconstruct a diffusion signal intrinsically continuous, and verifying  $E(\mathbf{0}) = 1$ . Besides, we define a Laplace regularization operator, and derive a method for its analytical computation.

## 2. METHODS

The functions  $B_{n,l,m}$  of the SPF basis [1] are expressed as the product of a real, symmetric spherical harmonic  $Y_{l,m}$  as

introduced in [2], and a radial function,

$$R_n(q) = \kappa_n L_n^{1/2} \left( \frac{q^2}{\zeta} \right) \exp \left( -\frac{q^2}{2\zeta} \right) \quad (1)$$

$$\kappa_n = \sqrt{\frac{2}{\zeta^{3/2}} \frac{n!}{\Gamma(n + 3/2)}}. \quad (2)$$

These functions are discontinuous about the origin, and we propose in this section to characterize a constraint to impose the continuity of a function expressed in this basis.

**Theorem 1** *A function  $f = \sum_{n,l,m} a_{n,l,m} B_{n,l,m}$  of the SPF basis is continuous if and only if*

$$\forall l > 0, \forall |m| \leq l, \sum_n a_{n,l,m} R_n(0) = 0. \quad (3)$$

The linear constraint in Eq. 3 can be imposed using constrained least squares minimization. Alternatively, we propose to reconstruct  $E(\mathbf{q}) - \exp(-\|\mathbf{q}\|^2/2\zeta)$  in a basis of continuous functions  $C_{n,l,m}$  verifying  $C_{n,l,m}(\mathbf{0}) = 0$ . Thus we impose the continuity, as well as  $E(\mathbf{0}) = 1$ .

### 2.1. A SPF basis modified for continuous signal

The functions of the modified SPF basis are defined as  $C_{n,l,m}(\mathbf{q}) = F_n(\|\mathbf{q}\|) Y_{l,m}(\mathbf{q}/\|\mathbf{q}\|)$ , where

$$F_n(q) = \chi_n \frac{q^2}{\zeta} L_n^{5/2} \left( \frac{q^2}{\zeta} \right) e^{-q^2/2\zeta}, \quad (4)$$

where  $L_n^{5/2}$  is the generalized Laguerre polynomial, and the normalization constant

$$\chi_n = \sqrt{\frac{2}{\zeta^{3/2}} \frac{n!}{\Gamma(n + 7/2)}}. \quad (5)$$

The family of functions  $C_{n,l,m}$  is an orthonormal basis, referred to as the modified SPF (mSPF) basis in what follows.

### 2.2. Relation between SPF and mSPF bases

The mSPF basis is compatible with the SPF basis, and we give in this section the explicit relation. This is important to

extend the results on analytical computation of the EAP and the orientation distribution function (ODF) [8] from the signal represented in the SPF basis, to the mSPF basis. Based on recurrence relations between Laguerre polynomials, the coefficients  $a_{n,l,m}$  and  $x_{n,l,m}$  in SPF and mSPF bases of a function are related through  $\mathbf{a} = \mathbf{M}\mathbf{x}$ , where  $\mathbf{M}$  is the change-of-basis matrix from mSPF to SPF.

$$M_{ij} = \delta_{l(i),l(j)}\delta_{m(i),m(j)} \cdot \begin{cases} \frac{3\chi_{n(j)}}{2\kappa_{n(i)}} & n(i) \leq n(j) \\ -\frac{n(i)\chi_{n(j)}}{\kappa_{n(i)}} & n(i) = n(j) + 1 \\ 0 & n(i) > n(j) + 1 \end{cases}$$

Besides, the matrix  $\mathbf{M}$  is orthogonal: the orthogonal projection of any function represented by its coefficients  $\mathbf{a}$  in the SPF basis, onto the subspace of continuous functions verifying  $f(\mathbf{0}) = 0$  has coefficients  $\mathbf{x} = \mathbf{M}^T \mathbf{a}$ .

### 2.3. Signal estimation with Laplace regularization

As the SNR in diffusion images is particularly low, we add a regularization constraint in coefficients estimation. The coefficients of  $E(\mathbf{q}) - \exp(-\|\mathbf{q}\|^2/2\zeta)$  in the mSPF basis are estimated minimizing

$$U(\mathbf{x}) = \|\mathbf{y} - \mathbf{B}\mathbf{x}\|^2 + \lambda \int_{\mathbb{R}^3} |\Delta E(\mathbf{q})|^2 d^3\mathbf{q}. \quad (6)$$

where  $y_i = E(\mathbf{q}_i) - \exp(-\|\mathbf{q}_i\|^2/2\zeta)$  and  $\mathbf{B}$  is the observation matrix. The Laplace penalization can be expressed simply as a quadratic form  $(\mathbf{x} - \mathbf{x}_0)^T \mathbf{\Lambda}(\mathbf{x} - \mathbf{x}_0) + U_0$ . In what follows, the constant term  $U_0$  is discarded as it plays no role in the minimization. The energy in Eq. 6 has a unique minimum  $\hat{\mathbf{x}} = \mathbf{x}_0 + (\mathbf{B}^T \mathbf{B} + \lambda \mathbf{\Lambda})^{-1}(\mathbf{y} - \mathbf{B}\mathbf{x}_0)$ . The entries of the matrix  $\mathbf{\Lambda}$  are

$$\Lambda_{i,j} = \delta_{l(i),l(j)}\delta_{m(i),m(j)} \int_0^\infty h_i(q)h_j(q) dq, \quad (7)$$

where

$$h_i = qF''_{n(i)} + 2F'_{n(i)} - \frac{l(i)(l(i)+1)}{q}F_{n(i)}. \quad (8)$$

The vector  $\mathbf{x}_0$  is given by  $\mathbf{x}_0 = -\mathbf{\Lambda}^{-1}\mathbf{v}$ , where the vector  $\mathbf{v}$  has entries

$$v_i = \delta_{l(i),0}\delta_{m(i),0} \int_0^\infty h_i(q) \left( \frac{q^3}{\zeta^2} - \frac{3q}{\zeta} \right) \exp\left(-\frac{q^2}{2\zeta}\right) dq. \quad (9)$$

The computation of  $\mathbf{\Lambda}$  and  $\mathbf{x}_0$  is analytical and needs no numerical integration. Indeed, the integrand  $h_i(q)h_j(q)$  can be written as  $\chi_{n(i)}\chi_{n(j)}/\zeta \exp(-q^2/\zeta)T_{i,j}(q^2/\zeta)$ , where  $T_{i,j}(X)$  is a polynomial. The coefficients  $a_k^{i,j}$  of  $T_{i,j}$  are computed using simple polynomial algebra. Therefore, the entries of the regularization matrix are

$$\Lambda_{i,j} = \frac{\chi_{n(i)}\chi_{n(j)}}{2\sqrt{\zeta}} \sum_{k=0}^d a_k^{i,j} \Gamma(k+1/2), \quad (10)$$

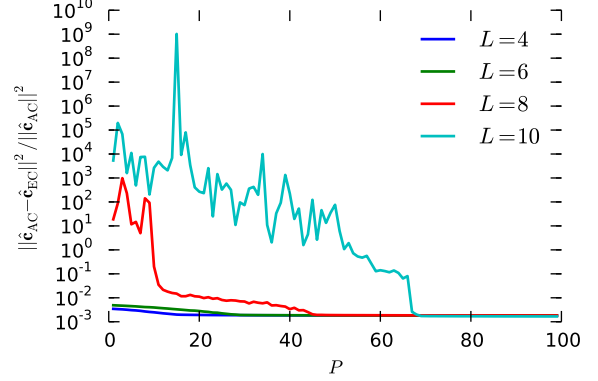


**Fig. 2.** Relative difference between reconstruction with analytical continuity (AC) constraint, and reconstruction with an empirical continuity (EC) constraint. Results on a synthetic Gaussian diffusion signal, from  $K = 150$  measurements on 3 Q-shells, plus  $P$  virtual measurements at  $\mathbf{q} = \mathbf{0}$ , for various angular orders  $L$  of the SPF basis.

### 2.4. Optimal regularization parameters

We adopted the Generalized Cross Validation (GCV) algorithm [3] to find the regularization weight  $\lambda$  which guarantees the best balance between the smoothness of the reconstruction, and the data fit. This algorithm has already been applied successfully for other applications in Q-ball diffusion MRI [4, 5]. The GCV method is generalizable to the situation where there is more than one  $\lambda$  parameter to optimize. It is the case in [1], where there are two regularization matrices  $\mathbf{N}$  and  $\mathbf{L}$ , which act respectively as radial and angular low-pass filters, with corresponding weights  $\lambda_N$  and  $\lambda_L$ .

## 3. EXPERIMENTS AND RESULTS

### 3.1. SPF and mSPF reconstruction

We compare on Fig. 1 the reconstruction in SPF and mSPF bases of a synthetic signal originating from a Gaussian EAP. The reconstruction in SPF basis was done with and without empirical continuity constraint. The sampling protocol is a set of 120 diffusion weighted measurements along 120  $\mathbf{q}$  vectors on 3 shells, with  $b$  values ranging from 1000 to 3000  $\text{s}\cdot\text{mm}^{-2}$ . It was designed following the method proposed in [6, 7].

We evaluate the difference of the signal reconstructed in mSPF basis (with exact continuity constraint), and compare it to the reconstruction with empirical continuity constraint. The coefficients of the former in SPF basis,  $\hat{c}_{AC}$ , are computed from the estimated coefficients in mSPF basis using the linear relation in Sec. 2.2. We plot on Fig. 2 the relative squared difference between both coefficient vectors  $\hat{c}_{AC}$  and  $\hat{c}_{EC}$ , where AC stands for analytical constraint, and EC for empirical constraint.

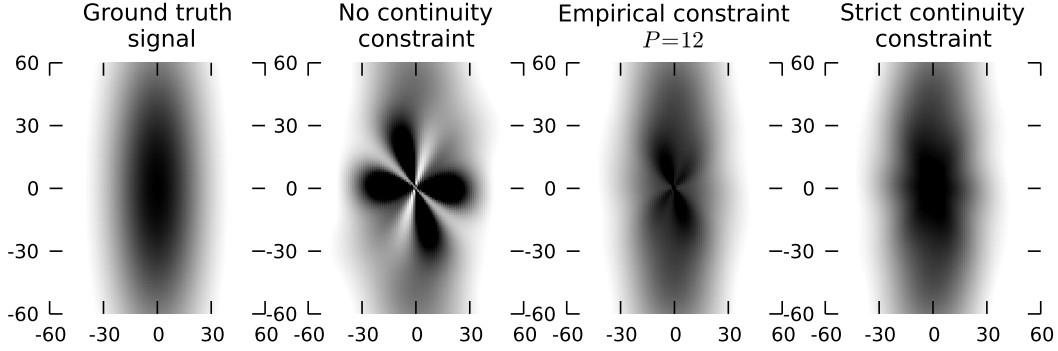


**Fig. 1.** Diffusion signal corresponding to a single fiber oriented along the  $x$ -axis, reconstructed from 120 samples in the  $Q$ -space. The signal is shown on the  $(q_x, q_y)$ -plane, and the grey levels correspond to signal range from 0.0 (white) to 1.0 (black).  $q$  values are understood in  $\text{mm}^{-1}$

As expected, the empirical solution converges to the analytical solution as the number of virtual measurements about 0,  $P$ , goes to infinity. However, the minimum value of  $P$  for an acceptable reconstruction is related to the angular order chosen. This makes the analytical solution better for all practical purposes.

### 3.2. Optimal Laplace regularization

We compare the reconstruction of the EAP and the orientation distribution function (ODF) computed following [8] with both regularization methods and plot the profiles on Fig. 3. The experiments were carried out on the publicly available phantom [9, 10]. The diffusion signal was sampled on 3  $Q$ -shells, with  $b$ -values ranging from 650 to  $2000 \text{ s} \cdot \text{mm}^{-2}$ , and 64 gradient directions per shell.

The Laplace regularization allows better reconstruction of fiber orientation, both in single fiber and crossing fibers configurations. The computational time for reconstruction was similar, however the minimization of the GCV function is much harder for the separate radial and angular filters, as a two-dimensional function is to be minimized. With no clue on the convexity of this function, we performed minimization using a grid search.

## 4. DISCUSSION AND CONCLUSION

In this work, we have addressed two problems related to the parametric reconstruction of the diffusion signal in the complete 3D  $Q$ -space. First, we have proposed an alternative basis, mSPF, to naturally impose the continuity of the diffusion signal on the whole space. This mathematical constraint results in a dimension reduction with respect to the SPF basis. Besides, the computational cost of the reconstruction in mSPF basis is also reduced, as no additional virtual measurements are needed to ensure continuity. In addition, we have derived the expression of a Laplace regularization operator

in this new basis. We have shown through generalized cross validation that Laplace regularization leads to a more accurate reconstruction than the commonly used low-pass filters. Moreover the latter acts separately on the radial and angular parts of the signal, hence the computation of optimal regularization weights is much simpler and computationally attractive with Laplace regularization, as we optimize on a single weight instead of two.

## 5. REFERENCES

- [1] H.E. Assemlal, D. Tschumperlé, and L. Brun, "Efficient computation of pdf-based characteristics from diffusion mr signal," *Medical Image Computing and Computer-Assisted Intervention*, no. 70–78, 2008.
- [2] M. Descoteaux, E. Angelino, S. Fitzgibbons, and R. Deriche, "Apparent diffusion coefficients from HARDI: Estimation and applications," *Magn Reson Med*, vol. 56, pp. 395–410, 2006.
- [3] P. Craven and G. Wahba, "Smoothing noisy data with spline functions," *Numerische Mathematik*, vol. 31, no. 4, pp. 377–403, 1985.
- [4] C. G. Koay, E. Özarslan, and P. J. Basser, "A signal transformational framework for breaking the noise floor and its applications in mri," *J Magn Reson*, vol. 197, no. 2, pp. 108–119, apr 2009.
- [5] Maxime Descoteaux, Cheng Guan Koay, Peter J. Basser, and Rachid Deriche, "Analytical q-ball imaging with optimal regularization," in *ISMRM 18th Scientific Meeting and Exhibition*, may 2010.
- [6] E. Caruyer, C. Lenglet, G. Sapiro, and R. Deriche, "Incremental gradient table for multiple q-shells diffusion mri," in *HBM 17th Annual Meeting*, Québec, Canada, jun 2011.
- [7] E. Caruyer, J. Cheng, C. Lenglet, G. Sapiro, T. Jiang, and R. Deriche, "Optimal design of multiple q-shells experiments for diffusion mri," in *MICCAI Workshop - CDMRI'11*, Toronto, Canada, sep 2011.
- [8] J. Cheng, A. Ghosh, R. Deriche, and T. Jiang, "Model-free, regularized, fast, and robust analytical orientation distribution function estimation," in *MICCAI*. 2010, vol. 6361 of *LNCIS*, pp. 648–656, Springer.
- [9] C. Poupon, B. Rieul, I. Kezele, M. Perrin, F. Poupon, and J-F. Mangin, "New diffusion phantoms dedicated to the study and validation of hardi models," *Magn Reson in Med*, vol. 60, pp. 1276–1283, 2008.
- [10] P. Fillard, M. Descoteaux, A. Goh, S. Gouttard, B. Jeurissen, J. Malcolm, A. Ramirez, M. Reisert, K. Sakaie, F. Tensaouti, T. Yo, J.F. Mangin, and C. Poupon, "Quantitative analysis of 10 tractography algorithms on a realistic diffusion MR phantom," *Neuroimage*, vol. 56, no. 1, pp. 220–234, 2011.

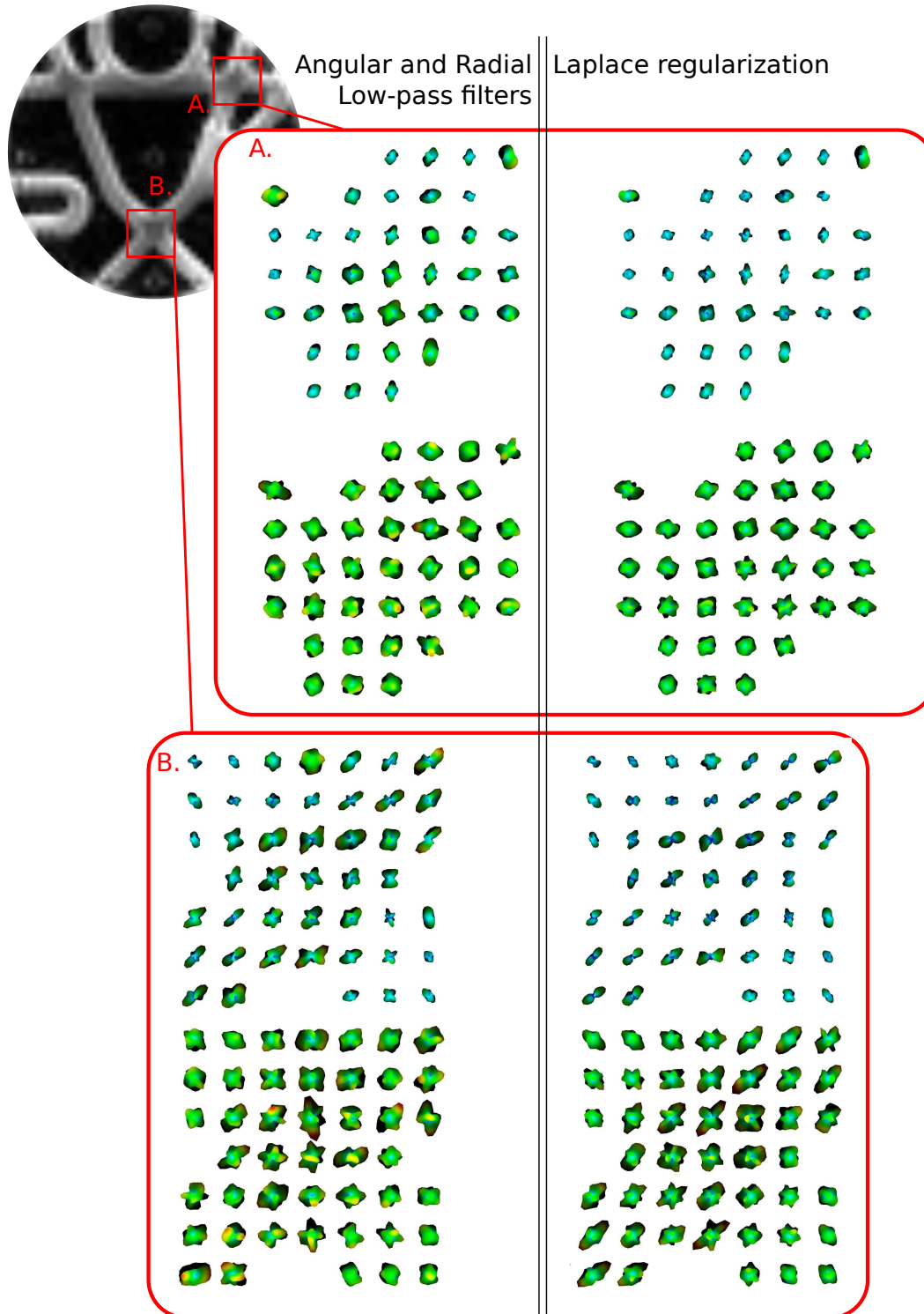


**Fig. 3.** Diffusion ODF and EAP profile reconstructed from the diffusion MRI data of the fiber cup. Zooms on crossing regions A and B are displayed. Within each block: EAP profile  $P(r_0 \mathbf{u})$ , for  $r_0 = 17 \mu\text{m}$  (top row) and diffusion ODF reconstructed in constant solid angle  $\psi(\mathbf{u})$ . The left column corresponds to a reconstruction with separate angular and radial low-pass filters, while the right column is the reconstruction with Laplace regularization.